

DISTANCE TO THE FORNAX CLUSTER USING THE HUBBLE SPACE TELESCOPE: IMPLICATIONS FOR COSMOLOGY

BARRY F. MA DORE¹, WENDY L. FREEDMAN², N. SILBERMANN⁴
ROBERT C. KENNICUTT Jr³, PAUL HARDING³, JEREMY R. MOULD⁵,
LAURA FERRARESE⁶, HOLLAND FORD⁶, JOHN A. GRAHAM⁷
MINGSHENG HAN⁸, JOHN G. HOESSEL³, JOHN HUCHRA⁹,
SHAUN M. HUGHES¹⁰, GARTH D. ILLINGWORTH¹¹, RANDY PHELPS²
SHOKO SAKAI⁴, PETER STETSON¹²

¹NASA/IPAC Extragalactic Database, Infrared Processing and Analysis Center,
Jet Propulsion Laboratory, California Institute of Technology, Pasadena, CA 91125

²Observatories of the Carnegie Institution of Washington, 813 Santa Barbara St.,
Pasadena, CA 91101

³Steward Observatory, University of Arizona, Tucson, AZ 85721

⁴Jet Propulsion Laboratory, California Institute of Technology, Pasadena, CA 91125

⁵Mt. Stromlo and Siding Spring Observatories, Institute of Advanced Studies, Private Bag,
Weston Creek Post Office, ACT 2611, Australia

⁶Space Telescope Science Institute, Homewood Campus, Baltimore, MD 21218

⁷Department of Terrestrial Magnetism, Carnegie Institution of Washington,
5241 Broad Branch Rd. N.W., Washington D.C. 20015

⁸Department of Astronomy, University of Wisconsin, 475 N. Charter St., Madison, WI 53706

⁹Smithsonian Institution, Center for Astrophysics, 60 Garden Street, Cambridge, MA 02138

¹⁰Royal Greenwich Observatory, Madingley Road, Cambridge, UK CB3 0HA

¹¹Lick Observatory, University of California, Santa Cruz, CA 95064

¹²Dominion Astrophysical Observatory, 5071 W. Saanich Rd., Victoria, BC, Canada V8X 4M6

ABSTRACT Using the **Hubble Space Telescope (HST)**, we have discovered **Cepheid variables** in the **Fornax cluster spiral galaxy, NGC 1365**. **V and I** period-luminosity relations for 37 Cepheids with periods between 12 and 60 days give a true modulus of $\mu_o = 31.43 \pm 0.06$ mag, corresponding to a distance of 19.3 ± 0.6 Mpc. Associating this distance with the Fornax cluster as a whole, and adopting a mean recessional velocity of $1,318 \pm 39$ km/sec (corrected to the barycentre of the Local Group and for Virgocentric flow) gives a local **Hubble constant** of $H_o = 68 \pm 7$ km/sec/Mpc. The quoted random error is 10%, while the largest systematic uncertainty is the currently (unknown) largescale-flow correction to the cosmological velocity of the cluster.

Seven Cepheid-based distances to groups of galaxies out to and including the Virgo and Fornax clusters yield $H_o = 70 \pm 3$ km/sec/Mpc. Recalibrating the Tully-Fisher relation using NGC 1365 and 6 nearby spiral galaxies, applied to 15 clusters out to 100 Mpc gives $H_o = 75 \pm 2$ km/sec/Mpc. A broad-based set of differential moduli established from Fornax out nearly a factor of ten in distance further, to **Abell 2147**, gives $H_o = 72 \pm 1$ km/sec/Mpc. With the addition of two Type Ia supernova calibrators in Fornax and correcting the supernova peak luminosities for decline rate, gives $H_o = 68 \pm 5$ km/sec/Mpc, out to a distance in excess of 500 Mpc. These major distance determination methods agree to within their statistical errors. **The resulting value** of the **Hubble constant**, encompassing all those determinations which are based on Cepheids and tied to secondary distance indicators out to **cosmologically** significant distances, is found to be 72 ± 2 km/sec/Mpc (random error, one sigma). Systematic uncertainties still exist at the 10% level (one sigma).

INTRODUCTION Although Hubble announced his discovery [1=H1] of the expansion of the Universe in 1929, decades of improvements in the measurement of extragalactic distances failed to converge on a consistent result. The improved resolution of the Hubble Space Telescope and consequent ability to discover classical Cepheid variables at distances a factor of ten further than can routinely be achieved from the ground, combined with a number of methods for measuring relative distances (from the ground) offers the promise to break the impasse.

It was clear soon after the December 1993 HST servicing mission that the discovery of Cepheids in the Virgo cluster (part of the original design specifications for the telescope), was feasible [2=F94]. Although the discovery of Cepheids in the Virgo cluster [3=F99] was an important step in resolving outstanding differences in the extragalactic distance scale, the Virgo cluster is complex both in its geometric and its kinematic structure, and there remain large uncertainties in both the velocity and distance to this cluster. Virgo clearly is not the ideal test site for an unambiguous determination of the cosmological expansion rate of the Universe.

NGC 1365 AND THE FORNAX CLUSTER The next major clustering of galaxies is the Fornax cluster. It is comparable in distance to the Virgo cluster [4=deV75], but found almost opposite to it in the sky of the southern hemisphere. Fornax is less rich in galaxies than Virgo [5=F88], but it is also substantially more compact than its northern counterpart (Figure 1). As a result of its lower mass, the influence of Fornax on the local velocity field is less dramatic than that of the Virgo cluster. And because of its compact nature, questions concerning the membership of individual galaxies in Fornax are less problematic, while the back-to-front geometry is far less controversial than any of these same points raised in the context of the Virgo cluster complex. Clearly, Fornax is a much more interesting site for a test of the local expansion rate.

Although the goals of the Key Project on the Extragalactic Distance Scale [6=K9] are far broader than just investigating the distances to a few nearby clusters, there are several important reasons to have a distance to the Fornax cluster. It is both a probe of the local expansion velocity field, and it is a major jumping-off point for a variety of secondary distance indicators which can be used to probe a volume of space at least 1,000 times larger. To secure a distance to Fornax, the Key Project is configured to monitor three galaxies in the cluster: the first of these, discussed here, is the strikingly picturesque, two-armed, barred-spiral galaxy, NGC 1365. In the coming year, the additional galaxies NGC 1425 and NGC 1326A are slated for observing.

At least three lines of evidence suggest that NGC 1365 is a member of the Fornax cluster. First, NGC 1365 is almost directly along our line of sight to Fornax. It is projected only ~ 70 arcmin from the geometric center of the cluster whereas the diameter of the cluster is ~ 200 arcmin [7=F89] (see Figure 1). In addition, NGC 1365 is also coincident with the Fornax cluster in velocity space. The systemic (heliocentric) velocity and velocity dispersion of the main population of galaxies in Fornax are well defined: 30 spirals/irregular galaxies give $\sigma = \pm 347$ km/see, 70 E/SO galaxies give $\sigma = \pm 335$ km/see, and the combined sample gives $\sigma = \pm 340$ km/see. The observed velocity of NGC 1365 (+1,636 km/see) is only +181 km/see larger than the mean velocity of the Fornax cluster as a whole, which based on 100 galaxies is found to be $1,455 \pm 34$ km/see [cf., 8=Sch96, 9=SR97, 10=HM90, NED]; with the mean velocity of the spirals agreeing with the mean for the elliptical to within 60 km/see). The velocity off-set of NGC 1365 is only half of the cluster velocity dispersion. Finally, we note that for its rotational velocity NGC 1365 sits only 0.02 mag from the central ridge line of the *apparent* Tully-Fisher relation relative to other cluster members defined by recent studies of the Fornax cluster [11=B96, 8=Sch96].

On the other hand, it is often noted that NGC 1365 is impressively large in its angular size, and that it is very bright in apparent luminosity as compared to any other galaxy in the immediate vicinity of the Fornax cluster. However, corrected for an inclination of 44° , the 21cm neutral hydrogen line width of NGC 1365 is found to be ~ 575 km/sec [11=B96,12=M9]. Using the Tully-Fisher relation as a *relative* guide to intrinsic size and luminosity, this rotation rate places NGC 1365 among the most luminous galaxies in the local (universe: brighter than M31 or M81, and comparable to NGC 4501 in the Virgo cluster or NGC 3992 in the Ursa Major cluster). We therefore conclude that NGC 1365 is in all respects apparently normal, (albeit large and luminous) and that its distance is consistent with it being a part of the ensemble of other elliptical and spiral galaxies constituting the Fornax cluster.

HST OBSERVATIONS Using the *Wide Field and Planetary Camera 2* on HST, we have obtained a set of 12-epoch observations of NGC 1365. These observations were begun on August 6, and continued until September 24, 1995. The observing window of 44 days was selected to maximize target visibility, without necessitating any roll of the targeted field of view. Sampling within the window was prescribed by a power-law distribution, tailored to optimally cover the light and color curves of Cepheids with anticipated periods in the range 10 to 60 days (see [3=F99] for additional details). Contiguous with 4 of the 12 V-band epochs, I-band exposures were also obtained so as to allow reddening corrections for the Cepheids to be determined. Each V-band epoch made use of the F555W filter and consisted of two exposures split between orbits (and allowing for cosmic ray rejection); a total of 5,100 sec of V-band data were obtained at each epoch in the course of the monitoring programme. The I-band exposures (F814W) totaled 5,400 sec each, again cosmic-ray split and accumulated over two orbits.

All frames were pipeline pre-processed at the *Space Telescope Science Institute* in Baltimore and subsequently analyzed in Pasadena using ALLFRAME (a suite of special-purpose stellar photometry packages [13=Ste94]). A second independent reduction is being performed using the DoPhot photometry package. The photometry from these two analyses agrees to within the errors discussed later. Zero-point calibrations for the photometry were adopted from [13a=ho9*] Holtzman *et al.* and from [14=H97], which agree to 0.05 mag on average. Details on the reduction and analysis of this data set are presented in [15=Sil97].

CEPHEIDS IN NGC 1365 Representative light curves for 18 of the 37 Cepheids discovered in NGC 1365 are given in Figure 2. As can be seen the phase coverage in all cases is sufficiently dense and uniform that the form of the light curves is clearly delineated. This allows these variables to be unambiguously classified as Cepheids with their distinctively rapid brightening, followed by a long linear decline phase. Mean magnitudes were obtained by weighting the individual observations by the semi-interval subtended by each phase point, averaged in intensity space, and transformed back into magnitudes. Periods used for phasing the data were obtained using a modified Lafler-Kinman algorithm [16=LK65]. The periods are judged to be (randomly) good to a few percent, although in some cases ambiguities larger than this do exist as a consequence of the narrow observing window and the restricted number of cycles (between 1 and 5) covered within the 44-day window.

The resulting V and I period-luminosity relations for the complete set of 37 Cepheids are shown in the upper and lower panels of Figure 3, respectively. The solid line is a minimum χ^2 fit to the fiducial PL relation for LMC Cepheids [17=M3], corrected for $E(B-V)_{\text{LMC}} = 0.10$ mag, scaled to an LMC true distance modulus of $\mu_0 = 18.50$ mag, and shifted into registration with the Fornax data. [Recent results from the Hipparcos satellite bearing on the Galactic calibration of the Cepheid zero point [17a, 17b] indicate that the LMC calibration is confirmed at the level of uncertainty indicated in Table 1, with the possibility that a small (upward) correction to the LMC reddening

is in order.] The derived apparent moduli are $\mu_V = 31.67 \pm 0.05$ mag and $\mu_I = 31.57 \pm 0.04$ mag. Correcting for a derived total line-of-sight reddening of $E(V-I)_{N1365} = 0.10$ mag (based on the Cepheids themselves) gives a true distance modulus of $\mu_0 = 31.43 \pm 0.06$ mag. This corresponds to a distance to NGC 1365 of 19.3 ± 0.6 Mpc. The quoted error *at this step in the analysis* quantifies only the statistical uncertainty generated by photometric errors in the data combined with the intrinsic magnitude and colour width of the Cepheid instability strip.

THE HUBBLE CONSTANT

We now discuss the impact of a Cepheid distance to Fornax in estimating the general expansion rate of the Universe. Below we present and discuss three independent estimates, where the analysis that follows is based on the Fornax distance and distances to other Key Project galaxies. At the end we intercompare the results for convergence and consistency. The first estimate is based solely on the Fornax cluster, its velocity and its Cepheid-based distance. This scrutinizes the flow sampled in one particular direction at a distance of ~ 20 Mpc. We then examine the inner volume of space, leading up to and including both the Virgo and Fornax clusters. This has the added advantage of averaging over different samples and a variety of directions, but it is still limited in volume (to an average distance of ~ 10 Mpc), and it is subject to the usual caveats concerning bulk flows and the adopted Virgocentric flow model. The third estimate comes from using the Cepheid distance to Fornax to lock into secondary distance indicators, thereby allowing us to step out to cosmologically significant velocities (10,000 km/sec and beyond) corresponding to distances greater than 100 Mpc. Local flow uncertainties then are replaced by large scale flow uncertainties; while the systematically secure Cepheid distances are replaced by currently more controversial secondary distance indicators. This is done in order to increase volume and the sample. Averaging over the sky, and working at large redshifts, alleviates the flow problems. Examining consistency between independent the secondary distance estimates, and then averaging over their far-field estimates should provide a systematically secure value of H_0 and, more importantly, a measure of its external error. Comparison of the three ‘regional’ estimates

(Fornax, local and far-field) then can be used to provide a check on the systematics resulting from the various assumptions made independently at each step.

THE HUBBLE CONSTANT AT FORNAX

Uncertainties in the Fornax Cluster Distance and Velocity: (1) Distance The two panels of Figure 1 show a comparison of the Virgo and Fornax clusters of galaxies drawn to scale, as seen projected on the sky. The comparison of apparent sizes is appropriate given the the two clusters are at approximately the same distance from us. In the extensive Virgo cluster, the galaxy M 100 can be seen marked $\sim 4^\circ$ to the north-west of the elliptical-galaxy-rich core: this corresponds to an impact parameter of 1.3 Mpc, or 8% of the distance from the LG to the Virgo cluster. The Fornax cluster is more centrally concentrated than Virgo, so that the back-to-front uncertainty associated with its three-dimensional spatial extent is reduced for any randomly selected member. Roughly speaking, converting the total angular extent of the cluster on the sky (~ 3 degrees in diameter; [7=F89]) into a back-to-front extent, the error associated with any randomly chosen galaxy in Fornax, translates into a few percent uncertainty in distance, and uncertainty in distance will soon be reduced when the two additional Fornax spirals are observed with HST in the coming year.

(2) Velocity Here, we note that the infall-velocity correction for the Local Group motion with respect to the Virgo cluster (and its associated uncertainty) becomes a minor issue for Fornax. This is the result of a fortuitous combination of geometry and physics. We now have Cepheid distances from the Local Group to both Fornax and Virgo. Combined with their angular separation on the sky this immediately leads to the physical separation between the two clusters proper. Under the assumption that the Virgo cluster dominates the local velocity perturbation field at the Local Group and at Fornax, we can calculate the velocity perturbation at Fornax (assuming that the flow field amplitude scales with $1/R_{\text{Virgo}}$, as first detailed by [18=Sche80] and characterized by a R^{-2}

density distribution). From this we then derive the flow contribution to the measured line-of-sight radial velocity as seen from the Local Group. Figure 4 shows the distance scale structure (left panel) and the velocity-field geometry (right panel) of the Local Group–Virgo–Fornax system. Adopting an infall velocity of the Local Group toward Virgo of $+200$ km/sec [for example 10=HM90, and following] with an uncertainty of ± 100 km/sec, the flow correction for Fornax is only -47 ± 23 km/sec.

(3) H_0 at Fornax, and its Uncertainties: Following the above discussion we calculate that the cosmological expansion rate of Fornax (as seen from the barycentre of the Local Group) is $1,318$ km/sec. Using our Cepheid distance of 19.3 Mpc for Fornax gives $H_0 = 68 (\pm 7)_r [\pm 17]_s$ km/sec/Mpc. The first uncertainty (in parentheses) includes random errors in the distance derived from the PL fit to the Cepheid data, as well as random velocity errors in the adopted Virgocentric flow, combined with the distance uncertainties to Virgo propagated through the flow model. The second uncertainty (in square brackets) quantifies the currently identifiable systematic errors associated with the adopted mean velocity of Fornax, and the adopted zero point of the PL relation (combining in quadrature the LMC distance error and a measure of the metallicity uncertainty). Finally, we note that according to the Han-Mould model [10], the Local Anomaly gives the Local Group an extra velocity component of approximately $+73$ km/sec towards Fornax. If we were to add that correction our local estimate for H_0 would increase to 72 km/sec/Mpc.

Given the highly clumped nature of the local universe and the existence of large-scale streaming velocities, there is still a lingering uncertainty about the total peculiar motion of the Fornax cluster with respect to the cosmic microwave background restframe. Observations of flows, and the determination of the absolute motion of the Milky way with respect to the background radiation suggest that line-of sight velocities ~ 300 km/sec are not uncommon [19=CL95]. The uncertainty in absolute motion of Fornax with respect to the Local Group then becomes the largest outstanding

uncertainty at this point in our error analysis: a 300 km/sec flow velocity for Fornax would result in a systematic error in the Hubble constant of $\sim 20\%$. We shall however be able to look from afar, and revisit this issue, following an analysis of more distant galaxies made later in this section.

THE NEARBY FLOW FIELD We now step back somewhat and investigate the Hubble flow between us and Fornax, derived from galaxies and groups of galaxies inside 20 Mpc, each having Cepheid-based distances and expansion velocities individually corrected for a Virgocentric flow model after [20=KK86]. Figure 5 captures those results in graphical form. At 3 Mpc the M81-NGC 2403 Group (for which both galaxies of this pair have Cepheid distance determinations) gives $H_0 = 75 \text{ km/sec/Mpc}$. Working further out to M101, the NGC 1023 Group and the Leo Group, the calculated values of H_0 range from 62 to 99 km/sec/Mpc. An average of these independent determinations including Virgo and Fornax, gives $H_0 = 70(\pm 3)_r \text{ km/sec/Mpc}$. This determination uses a Virgocentric flow model with a $1/R_{\text{Virgo}}$ infall velocity fall-off, scaled to a Local Group infall velocity of +200 km/sec, which was determined *ab initio* by minimizing the velocity residuals for the galaxies with Cepheid-based distances [as in 10=HM90],

The foregoing determination of H_0 is again predicated on the assumption that the inflow-corrected velocities of both Fornax and Virgo are not further perturbed by other mass concentrations or large-scale flows, and that the 2.5,000 Mpc³ volume of space delineated by them is at rest with respect to the distant galaxy frame. To avoid these local uncertainties we now step out from Fornax to the distant flow field. There we explore three applications: (1) Use of the Tully-Fisher relation calibrated by Cepheids locally, and now including NGC 1365 and about two dozen additional galaxies in the Fornax cluster. Ultimately these calibrators are tied into the distant flow field at 10,000 km/sec defined by the the Tully-Fisher sample of galaxies in clusters given by [21=AMH80]. (2) Using the distance to Fornax to tie into averages over previously published differential moduli for independently selected distant-field clusters, (3) Recalibrating the Type Ia supernova luminosities

at maximum light, and applying that calibration to events as distant as 30,000 km/sec.

BEYOND FORNAX: THE TULLY-FISHER RELATION Quite independent of its association with the Fornax cluster as a whole, NGC 1365 provides an important calibration point for the Tully-Fisher relation which links the (distance-independent) peak rotation rate of a galaxy to its Intrinsic luminosity. In the left panel of Figure 6 we show NGC 1365 in addition to NGC 925 [22=Sil96], NGC 4536 [26=A99] and NGC 4639 [27=S4639] added to the ensemble of calibrators having published Cepheid distances [28=F90]. As mentioned earlier NGC 1365 does now provide the brightest data point in the relation: additional galaxies soon to be added include NGC 2090 [23=P97], NGC 3351 [24=Gr97] and NGC 3621 [25=Ra97].

Although we have only the Fornax cluster for comparison at the present time, it is interesting to note that there is no obvious discrepancy in the Tully-Fisher relation between galaxies in the (low-density) field and galaxies in this (high-density) cluster environment. The NGC 1365 data point is consistent with the data for other Cepheid calibrators. Adding in all of the other Fornax galaxies for which there are published I-band magnitudes and inclination-corrected HI line widths provides us with another comparison of field and cluster spirals. In the right panel of Figure 6 we see that the 21 Fornax galaxies (shifted by the true modulus of NGC 1365) agree extremely well with the 9 brightest Cepheid-based calibrators. The slope of the relation is virtually unchanged by this augmentation; with the scatter about the fitted line increasing somewhat to ± 0.35 mag. (Nevertheless the small intrinsic scatter in the relation greatly diminishes the impact of Malmquist-bias.) In following applications we adopt $M_I = -8.80 \log(\Delta V - 2.445) + 20.48$ as the best-fitting least squares solution for the calibrating galaxies.

Han [29=H91] has presented I-band photometry and neutral-hydrogen line widths for the determination of Tully-Fisher distances to individual galaxies in 16 clusters out to redshifts exceeding 10,000 km/sec. We have rederived distances and uncertainties to each of these clusters

using the above-calibrated expression for the Tully-Fisher relation. The results are contained in Figure 7. A linear fit to the data in Figure 7 gives a Hubble constant of $H_0 = 75 \text{ km/sec/Mpc}$ with a total observed scatter giving a formal (random) uncertainty on the mean of only $\pm 2 \text{ km/sec/Mpc}$. It is significant that neither Fornax nor Virgo deviate to any significant degree from an inward extrapolation of this far-field solution. At face value, these results provide evidence for both of these clusters having only small motions with respect to their local Hubble flow.

BEYOND FORNAX: OTHER RELATIVE DISTANCE DETERMINATIONS

In addition to the relative distances compiled using the Tully-Fisher relation discussed above, Jergen and Tammann [30=JT93] have compiled a set of relative distance moduli based on a number of independent secondary distance indicators, including brightest cluster galaxies, Tully-Fisher and supernovae. We adopt, without modification, their differential distance scale and tie into the Cepheid distance to the Fornax cluster, which was part of their cluster sample. The results are shown in Figure 8 which extends the velocity-distance relation out to more than 160 Mpc. No error bars are given in the published compilation but it is clear from the plot that the observed scatter is fully contained by 10% errors in distance or velocity. This sample is now sufficiently distant to average over the potentially biasing effects of large-scale flows, and yields a value of $H_0 = 72(\pm 1)_r \text{ km/sec}$ (random), with a systematic error of 10% being associated with the distance (but not the velocity) of the Fornax cluster. Again the coincidence of H_0 at Fornax with that for the far field, argues for Fornax being relatively at rest with respect to the microwave background.

BEYOND FORNAX: TYPE Ia SUPERNOVAE

In a separate paper [31=Fre97] details are reported on the impact of a Cepheid distance to Fornax specifically on the calibration and application of Type Ia supernovae to the extragalactic distance scale. Various calibrations dealing with interstellar extinction and/or decline-rate correlations are presented. Application to the distant Type Ia supernovae of [32=Ham96] gives $H_0 = 68 \text{ km/sec/Mpc}$.

COSMOLOGICAL IMPLICATIONS Given the consistency of Hubble constants derived, both locally and at large recessional velocities, then we can state that H_0 falls within the full-range extremes of 75 ± 1 and 68 ± 5 km/sec/Mpc, giving formally $H_0 = 72(\pm 2)_r [\pm 10]_s$ km/sec/Mpc out to a velocity-distance $O. 1c$ (30,000 km/sec.) These results are summarized graphically in Figure 9 and numerically in Table 3.

A value of the Hubble constant, in combination with an independent estimate of the average density of the Universe, can be used to estimate a dynamical age for the Universe (*e.g.*, see Figure 10). For a value of $H_0 = 72(\pm 2)_r$ km/sec/Mpc, the age ranges from a high of ~ 12 Gyr for a low-density ($\Omega = 0.2$) Universe, to a young age of ~ 9 Gyr for a critical-density ($\Omega = 1.0$) universe.

Other, independent constraints on the age of the Universe exist: most notably the ages of the oldest stars, as typified by Galactic globular clusters. These ages traditionally are thought to fall in the range of 14 ± 2 Gyr [33=Ch96], however the subdwarf parallaxes obtained by the Hipparcos satellite [34=R97] may reduce these ages considerably. Interpreted within the context of the standard Einstein-de Sitter model (having a cosmological constant of zero) our value of $H_0 = 72$ km/sec/Mpc, if constrained by the stellar ages, is incompatible with a high-density ($\Omega = 1.0$) model universe (at the 2.5-sigma level in the identified systematic errors.) For $\tau = 14$ Gyr, H_0 would have to be ~ 45 km/sec/Mpc if $\Omega = 1.0$.

ACKNOWLEDGEMENTS This research was supported by the National Aeronautics and Space Administration (NASA) and the National Science Foundation (NSF), and benefited from the use of the NASA/IPAC Extragalactic Database (NED). Observations are based on data obtained using the *Hubble Space Telescope* which is operated by the Space Telescope Science Institute under contract from the Association of Universities for Research in Astronomy.

REFERENCES

- [1=H1] Hubble, E. F. *Proc. Nat. Acad. Sci.*, **15**, 168-173 (1929).
- [2=F94] Freedman, W. L., Madore, B. F., Stetson, P. B., *et al.* *Astrophys. J.*, **435**, L31-L34 (1994).
- [3=F99] Freedman, W. L. *et al.* *Nature*, **371**, 757-762 (1994).
- [4=deV75] de Vaucouleurs, G., in *Stars and Stellar Systems*, 9. (ed. R. Sandage, M. Sandage, J. Kristian, eds.), Univ Chicago Press, 557-596. (1975).
- [5=F88] Ferguson, H.C. & Sandage, A.J. *Astr. J.*, **96**, 1520-1533 (1988).
- [6=K9] Kennicutt, R. C., Freedman, W.L. & Mould, J.R. *Astron. J.*, **110**, 1476-1491, (1995).
- [7=F89] Ferguson, H.C. *Astr. J.*, **98**, 367-418 (1989).
- [8=Sch96] Schroder, A. Doctoral Thesis, University of Basel (1995).
- [9=SR97] Schroder, A., & Richter, O.-G., in preparation, (1997).
- [10=HM90] Han M., & Mould J.R. *Astrophys. J.*, **360**, 448-464 (1990).
- [11=B96] Bureau, M., Mould, J. R., & Staveley-Smith, L. *Astrophys. J.*, **463**, 60-68 (1996).
- [12=M9] Mathewson, D. S., Ford, V. L., & Buchhorn, M. *Astrophys. J. Suppl.* **81**, 413-659 (1992).
- [13=Ste94] Stetson, P. B., *Publ. astron. Soc. Pacif.*, **106**, 250-280, (1994).
- [13A=Ho95] Holtzmann, *et al.* *Publ. astron. Soc. Pacif.*, **107**, 156-173, (1995).
- [14=H97] Hill, R. *et al.* *Astrophys. J. Suppl.*, in press (1997).
- [15=Sil97] Silbermann, N.A., Harding, P., Madore, B. F. *et al.* *Astrophys. J.*, in preparation (1997).
- [16=LK65] Lafler, J., & Kinman, T.D. *Astrophys. J. Suppl.*, **11**, 216-222 (1965).
- [17=M3] Madore, B.F. & Freedman, W.L. *Publ. astron. Soc. Pacif.*, **103**, 933-957 (1991).
- [17a] Feast, M. W., & Catchpole, R.M. *M. N. R. A. S.*, in press (1997).

- [17b]Madore, B. F. & Freedman, W.L. *Astrophys. J. (Lett.)*, submitted (1997).
- [18=Sche80]Schechter, P. *Astron. J.*, 85, 801-811 (1980)
- [19=CL95] Coles, P.. & Lucchin, F..In *Cosmology*, Wiley, 399-400, (1995)
- [20= KK86] Kraan-Korteweg, R., *Astron. Astrophys. Suppl.*66, 255-279. (19S6).
- [21=AMH80]Aaronson, M., Mould, J., Huchra, J., Houck I, J., Sullivan, W. T., Schommer, R.A. & Bothun, G.D. *Astrophys. J.*, 239, 12-37 (1980).
- [22=Sil96] Silbermann, N., *et al. Astrophys. J.*, 470. 1-37 (1996).
- [23=P97] Phelps, R., *et al. Astrophys. J.*, in preparation, (1997).
- [24=Gr97]Graham, J.A. *et al. Astrophys. J.*, 477535-559 (1997).
- [25=Ra97] Rawson, D.M. *et al. Astrophys. J.*, in preparation, (1997).
- [26=A99] Saha, .A., Sandage, A. R., Labhardt, L., Tammann, G.A., Macchetto, F. D., & Panagia, N. *Astrophys. J.*, 466, 55-91 (1996).
- [27= S4639] Sandage, A. R., Saha, A., Tammann, G. A., Labhardt, L., Panagia, N. & Macchetto, F.D. *Astrophys. J. (Lett.)* 460, L15-18 (1996).
- [28=F90] Freedman, W.L. *Astrophys. J. (Lett.)*, 355, 1,35-1,38 (1990).
- [29= Han9] Han, M.S. *Astrophys. J. Suppl.*, 81, 35-48 (1992).
- [30=JT93] Jerjen, H., & Tammann, G.A. *Astr. .Ap.*, 276, 1-8 (1993).
- [31=Fre97] Freedman, W.L. *et al.* in preparation (1997).
- [32= Ham96] Hamuy, M., *et al. Astrophys. J.*, (1996)
- [33= Ch96] Chaboyer, B., Demarque, P., Kernan, P.J. & Krauss, L.M. *Science*, 271, 957-961 (1996).
- [34= R97] Reid, N. *Ap. J. (Letters)*, submitted (1997)

FIGURE CAPTIONS

Figure 1. – A comparison of the distribution of galaxies as projected on the sky for the Virgo cluster (right panel) and the Fornax cluster (left panel). M100 and NGC1365 are each individually marked by arrows showing their relative disposition with respect to the main body and cores of their respective clusters. Units are arcmin.

Figure 2. – Representative V-band light curves for 18 of the 37 Cepheid variables found in the Fornax cluster galaxy, NGC1365.

Figure 3. – V and I-band Period-Luminosity relations for the full set of 37 Cepheids monitored in NGC1365. The fits are to the fiducial relations given by [17=M3] shifted to the apparent distance modulus of NGC 136.5. Dashed lines indicate the expected intrinsic (2-sigma) width of the relationship due to the finite temperature width of the Cepheid instability strip.

Figure 4. – Relative geometry (left panel), and the corresponding velocity vectors (right panel) for the disposition and flow of Fornax and the Local Group with respect to the Virgo cluster. The circles plotted at the positions of the Virgo and Fornax clusters have the same angular size as the circles minimally enclosing M100 and NGC 1365 in the two panels of Figure 1.

Figure 5. – The velocity-distance relation for local galaxies having Cepheid-based distances. Circled dots mark the velocities and distances of the parent groups or clusters. The one-sided “error” bars with galaxy names attached mark the velocities associated with the individual galaxies having direct Cepheid distances. The broken line represents a fit to the data giving $H_0 = 70 \pm 3$ km/sec/Mpc. The 95% confidence interval on the observed scatter is ± 1.4 km/sec/Mpc, and is shown by the thin diverging broken lines; the solid lines indicate one-sigma limits.

Figure 6. – Tully-Fisher relations. The left panel shows the absolute I-band magnitude, M_I versus the inclination-corrected 21-cm line widths for galaxies having individually determined Cepheid distances. NGC1365 is seen to be the brightest object in this sample, but the position of this *cluster spiral* is fully consistent with an extrapolation of the relation defined by the lower luminosity *field galaxy sample*. The right panel shows the calibrating sample (filled circles) superimposed on the entire population of Fornax spiral galaxies for which I-band observations and line widths are available: the latter being shifted to absolute magnitudes by the Cepheid distance to NGC 1365.

Figure 7. – The velocity-distance relation for 15 clusters of galaxies out to 11,000 km/sec, having distance moduli determined from the I-band Tully-Fisher relation. A fit to the data gives a Hubble constant of $H_0 = 75 \pm 2$ km/sec/Mpc. The solid lines mark one-sigma bounds on the observed internal scatter.

Figure 8. – The velocity-distance relation for 17 clusters of galaxies, having published [30=JT93] differential distance moduli scaled to the Fornax cluster. A fit to the data gives a Hubble constant of $H_0 = 72 \pm 1$ km/sec/Mpc. As in Figure 7, the solid lines mark one-sigma bounds on the observed internal scatter.

Figure 9. – A graphical representation of Table 3 showing the various determinations of the Hubble constant, and the adopted mean. Each value of H_0 is represented by a gaussian of unit area centred on its determined value and having a dispersion equal to the quoted *random* error. Superposed on each gaussian is a horizontal bar representing the one sigma limits of the calculated systematic *errors* derived for that determination. The adopted average value and its probability distribution function is the arithmetic sum of the individual gaussians.

Figure 10. – Lines of fixed time representing the theoretical ages of the oldest globular cluster stars are shown for 12, 14 and 16 Gyr, plotted as a function of the expansion rate H_0 and density parameter Ω_0 , for an Einstein-de Sitter universe with the cosmological constant $\Lambda = 0$. The dashed horizontal line at $H = 72$ is the average value of the Hubble constant given in Table 3. The parallel (solid) lines on either side of that solution represent the one-sigma random errors on that solution. Systematic errors on the solution for H_0 are represented by dashed lines at 62 and 82 km/sec/Mpc. The only region of (marginal) overlap between these two constraints is in the low density ($\Omega < 0.2$) regime, unless $\Lambda \neq 0$. If the globular cluster ages are assumed to place a *lower bound* on the age of the Universe, the region of plausible overlap between the two solutions is more severely restricted to even lower density models.

TABLE 1

ERROR, BUDGET THE CEPHEID DISTANCE TO NGC 1365

Source of Uncertainty on the Mean	Description of Uncertainty	Percentage Error
LMC	CEPHEID PL CALIBRATION	
[A] LMC True Modulus	Independent Estimates = 18.50 ± 0.15 mag	8%
[B] V PL Zero Point	LMC PL $\sigma_V = (0.27)/\sqrt{31} = \pm 0.05$ mag	3%
[C] I PL Zero Point	LMC PL $\sigma_I = (0.18)/\sqrt{31} = \pm 0.03$ mag	2%
[SC] Systematic Uncertainty	[A] + [B] + [C] combined in quadrature	8%
NGC 1365	CEPHEID TRUE DISTANCE MODULUS	
(D) HST V-Band Zero Point	On-Orbit Calibration: ± 0.05 mag	3%
(E) HST I-Band Zero Point	On-Orbit Calibration: ± 0.05 mag	3%
(M1) Cepheid True Modulus	[D][E] are uncorrelated, but coupled by reddening law: $\sigma_{\mu_o} = \pm 0.15$ mag	7%
(F) Cepheid V Modulus	NGC 1365 PL $\sigma_V = (0.27)/\sqrt{37} = \pm 0.05$ mag	3%
(G) Cepheid I Modulus	NGC 1365 PL $\sigma_I = (0.26)/\sqrt{37} = \pm 0.04$ mag	2%
(M2) Cepheid True Modulus	[F] and [G] are partially correlated, giving $\sigma_{\mu_o} = \pm 0.06$ mag	3%
[Z] Metallicity	M31 metallicity gradient test gives $\sigma_{\mu_o} = \pm 0.08$ mag	4%
(J) Random Errors	[M1] + [M2] combined in quadrature	8%
[K] Systematic Errors	[SC] + [Z] combined in quadrature	9%
	D = 19.3 Mpc ± 1.5 (random) ± 1.7 [systematic]	

Note: There are 32 Cepheids in the LMC with published VI photometry [17=MF91]. The measured dispersions in the period-luminosity relations at V and I are 0.27 and 0.18 mag, respectively.

TABLE 2

ERROR BUDGET ON THE HUBBLE CONSTANT

Source of Uncertainty on the Mean	Description of Uncertainty	Percentage Error
FORNAX CLUSTER EXPANSION VELOCITY AND INFERRED DISTANCE		
(L) Velocity Dispersion	$\pm 34 \text{ km/sec} = \pm 340 / \sqrt{N-1}$ (No. of galaxies = 100) at $\langle V \rangle = 1,318 \text{ km/sec}$	3%
(M) Geometry of Cluster	*O. -1 Mpc at 19.3 Mpc	2%
[N] Virgo-centric Flow	$\pm 20 \text{ km/sec}$ on -40 km/sec along the Local Group line of sight (see text)	1%
[O1] Bulk Flow	$\pm 300 \text{ km/sec}$	23%
Random Errors	(J) + (L) + (M) combined in quadrature	10%
Systematic Errors	[K] + [N] + [O1] combined in quadrature	25%
	$H_0 = 68 \text{ km/sec/Mpc} \pm 7$ (random) ± 17 [systematic]	
LOCAL FLOW M81, M101, N2090, N3621, N7331, VIRGO, FORNAX		
(P) Random Motions	$\pm 2 \text{ km/sec/Mpc} = \pm 8 / \sqrt{N-1}$ (so of galaxies = 7)	4%
[O2] Bulk Flow	$\pm 300 \text{ km/sec}$ at $V(\text{max}) = +1, -100 \text{ km/sec}$	21%
Random Errors	(P) = total observed scatter	4%
Systematic Errors	[SC] + [Z] + [O2] combined in quadrature	23%
	$H_0 = 70 \text{ km/sec/Mpc} \pm 3$ (random) ± 16 [systematic]	
DISTANT FLOW I. TULLY-FISHER: 16 CLUSTERS TO 10,000 km/sec		
(S) Observed Scatter	$\pm 0.04 \text{ mag} = \pm 0.16 / \sqrt{N-1}$ (No. of clusters = 16)	2%
[R] TF Zero Point	$\sigma(\text{mean}) = \pm 0.13 \text{ r-mag} = \pm 0.40 / \sqrt{N-1}$ (No. of calibrators = 11)	6%
[O3] Bulk Flow	$\pm 300 \text{ km/sec}$ evaluated at 10,000 km/sec	3%
Random Errors	(s)	2%
Systematic Errors	[SC] + [Z] + [R] + [O3] combined in quadrature	11%
	$H_0 = 75 \text{ km/sec/Mpc} \pm 2$ (random) ± 8 [systematic]	
DISTANT FLOW II. HYBRID METHODS: 17 CLUSTERS TO 11,000 km/sec		
(U) Observed Scatter	$\pm 0.02 = \pm 0.06 / \sqrt{N-1}$ (No. of clusters = 17)	2%
[O4] Bulk Flow	$\pm 300 \text{ km/sec}$ evaluated at 11,000 km/sec	3%
[1] Fornax Distance	[SC] + [Z] combined in quadrature	10%
Random Errors	(U)	2%
Systematic Errors	[1] = [Se] t [0'1] t [z]	10%
	$H_0 = 72 \text{ km/sec/Mpc} \pm 1$ (random) ± 7 [systematic]	
DISTANT FLOW III. Type Ia SN: 20 EVENTS OUT TO 20,000 km/sec		
(T1) Peak Luminosity	$\pm 0.11 \text{ mag} = \pm 0.45 / \sqrt{N-1}$ (No. of SNIa = 16)	6%
(V1) Random Motions	$\pm 300 \text{ km/sec}$ at 5,000 km/sec	6%
[0.5] Bulk Flow	$\pm 300 \text{ km/sec}$ at 20,000 km/sec	2%
[Q1] SNIa Zero Point	$\sigma(\text{mean}) = \pm 0.18 \text{ mag} = \pm 0.45 / \sqrt{N-1}$ (No. of calibrators = 7)	9%
Random Errors	(T1) + (Vi) combined in quadrature	8%
Systematic Errors	[SC] + [05] + [Q1] combined in quadrature	19%
	= 68 (random) [systematic]	

TABLE 3
SUMMARY

Method	Hubble Constant (Random)	[Systematic]
Fornax Cluster	68 km/sec/Mpc ± 7 (random)	± 18 [systematic]
Local Flow	70 km/sec/Mpc ± 3 (random)	± 16 [systematic]
Tully-Fisher	75 km/sec/Mpc ± 2 (random)	± 8 [systematic]
Hybrid Methods	72 km/sec/Mpc ± 1 (random)	± 7 [systematic]
Type 1a SNe	68 km/sec/Mpc ± 5 (random)	* 8 [systematic]
Modal Average:	72 km/sec/Mpc ± 3 (random)	*10 [systematic]
Major Systematics:	$\pm 10\%$ [FLOWS] $\pm 8\%$ [LMC]	$\pm 4\%$ [Fe/H]

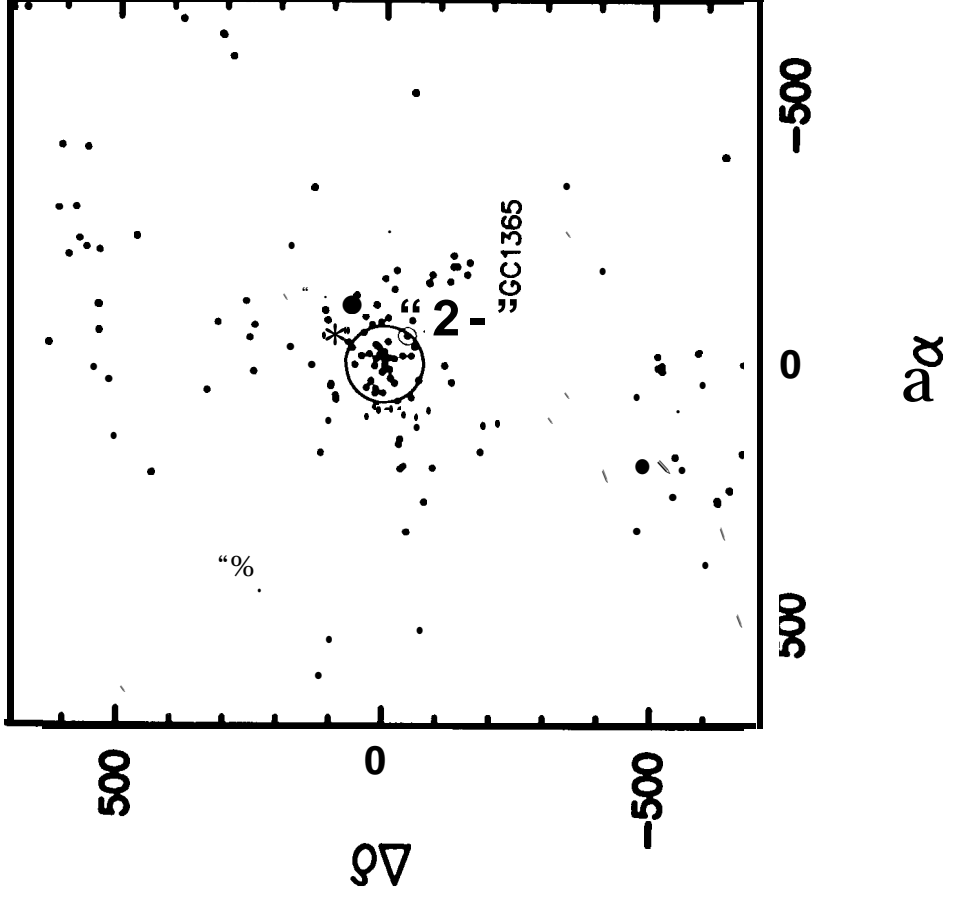
Notes: (1) The measured scatter of the $N = 5$ tabulated values of the Hubble constant about the derived mean of 72 km/sec/Mpc is ± 3 km/sec/Mpc; the formal error on the mean (due to random errors) is then $3/\sqrt{N-1} = 1.5$ km/sec/Mpc.

(2) The systematic error due to large-scale flows is the average of the ± 300 km/see term on each of the five methods. (2370, 21%, 3%, 370 and 1%, respectively, as given in Table 2)

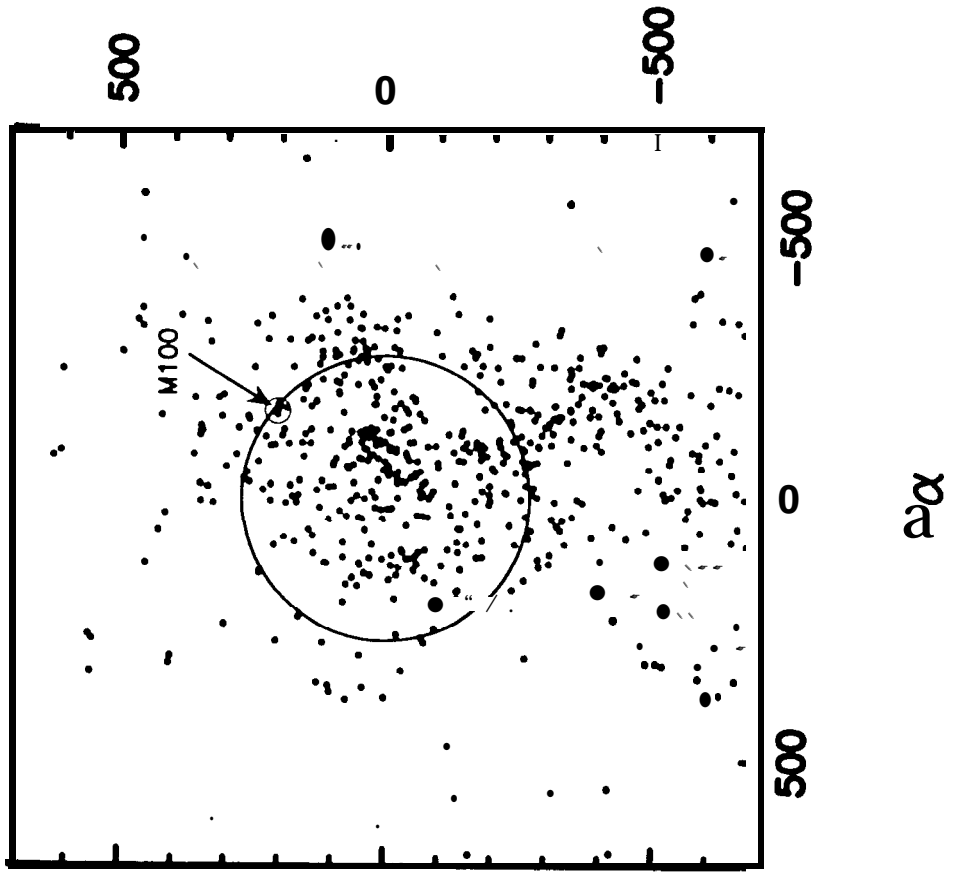
(3) Calculated for differences in the five Hubble constants with respect to the mean, and scaled to their externally quoted errors, the reduced $\chi^2 = 0.78$. This is only slightly smaller than expected by chance, and suggests that the random errors on the individually determined values of the Hubble constant are realistic.

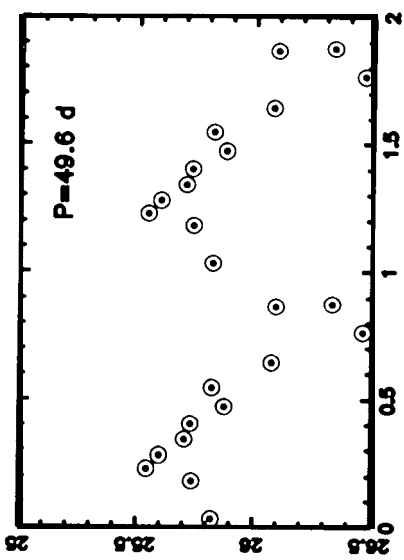
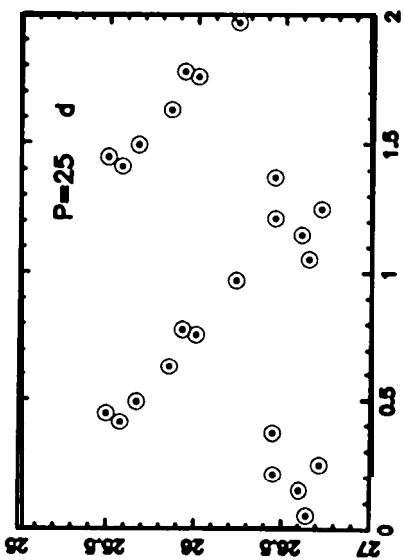
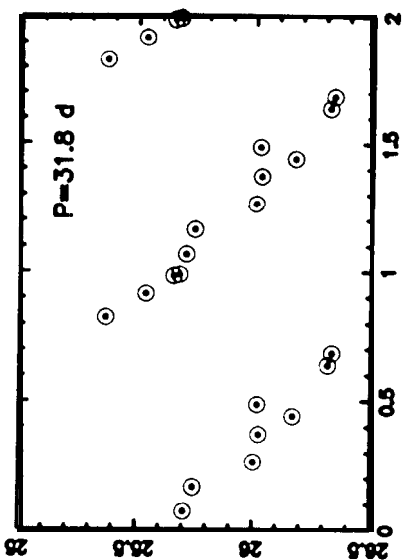
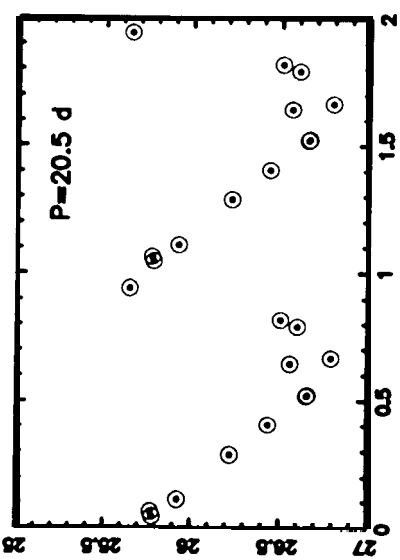
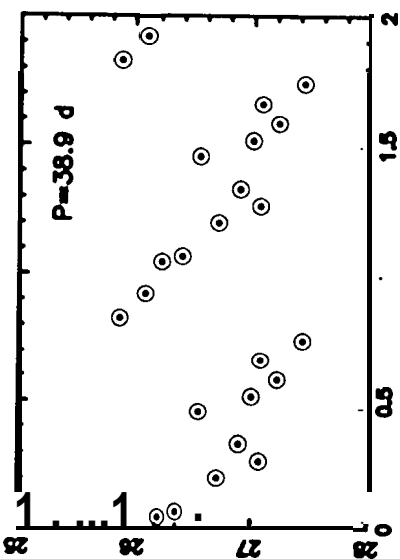
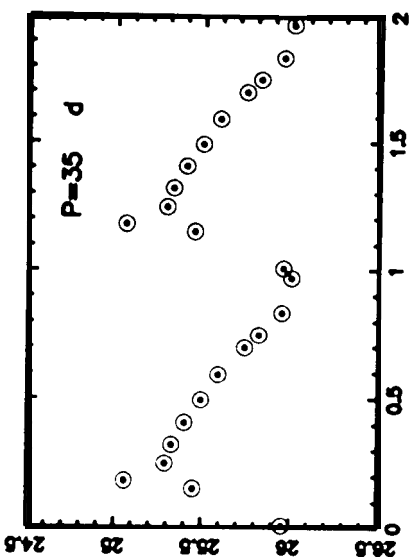
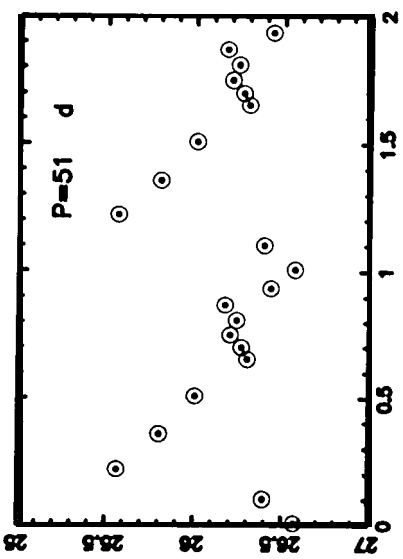
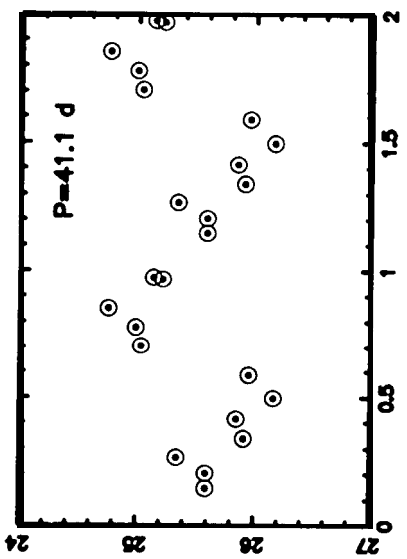
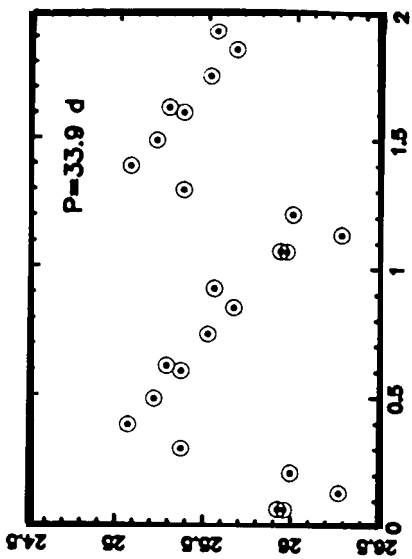
(4) The concordance between the local and far-field values of the the Hubble constant argue that there is no large flow of the local supercluster with respect to the 20,000 km/see volume probed by the SNe. At face value the differences in Hubble constants admit a local flow of ~ 85 km/see. If so, the (averaged) systematic error due to large scale flow perturbations drops from a dominant 10% down to 4%, leaving the LMC distance as the leading source of systematic error on H_0 .

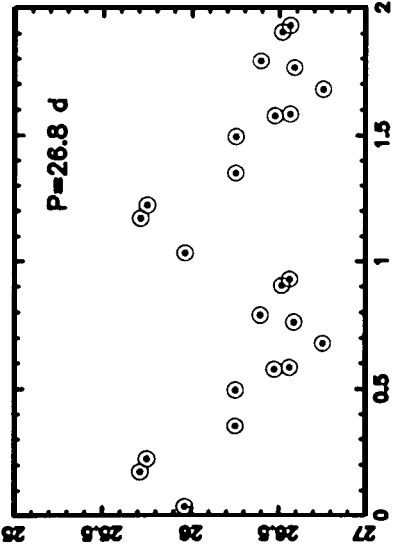
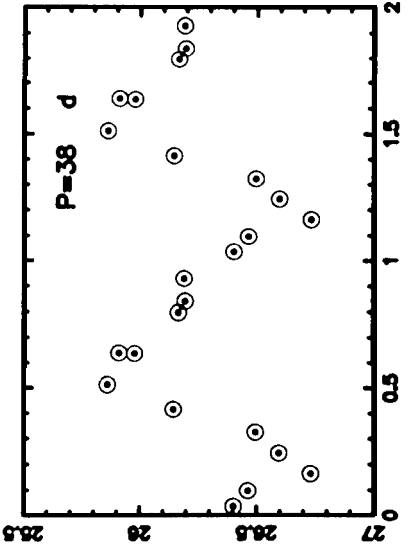
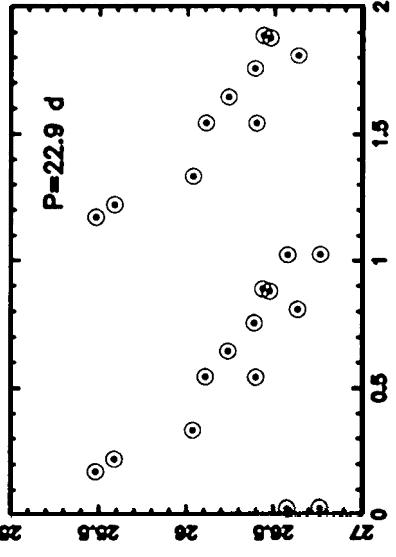
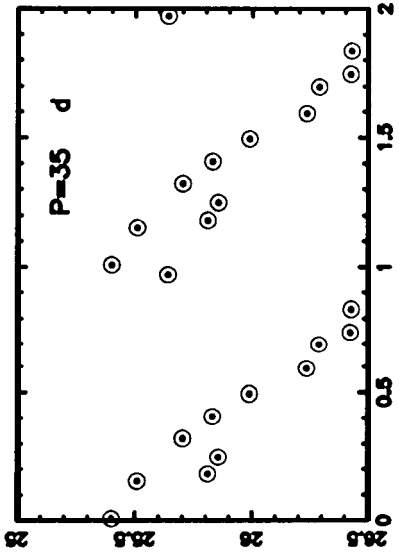
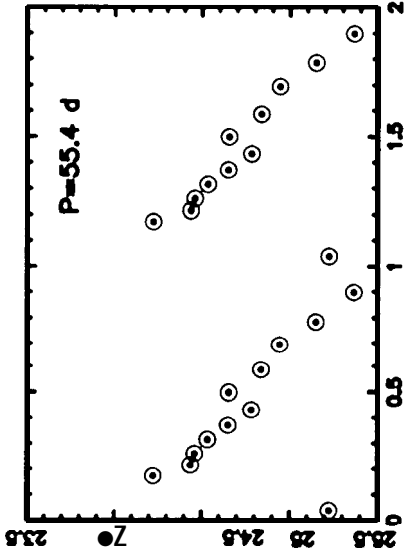
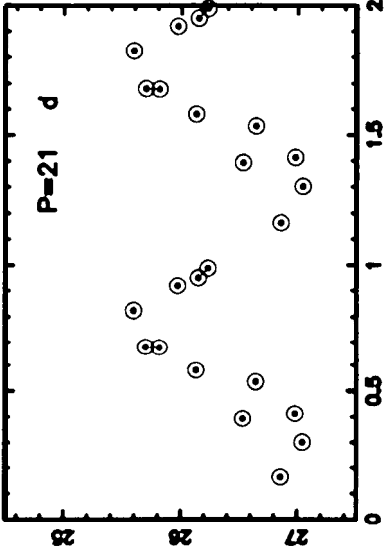
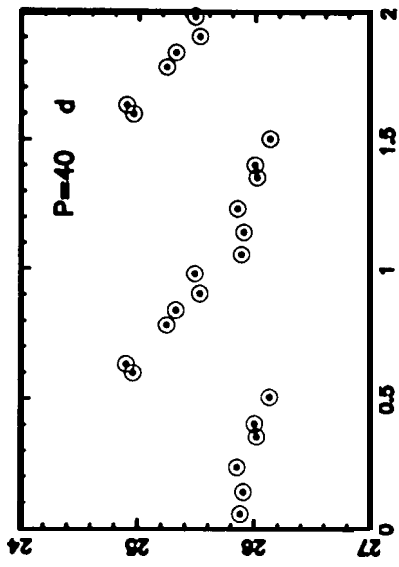
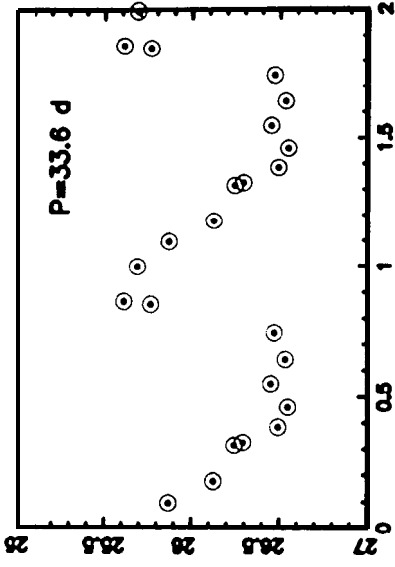
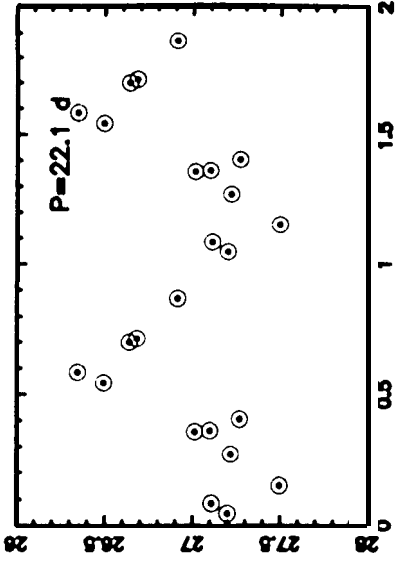
FORNAX



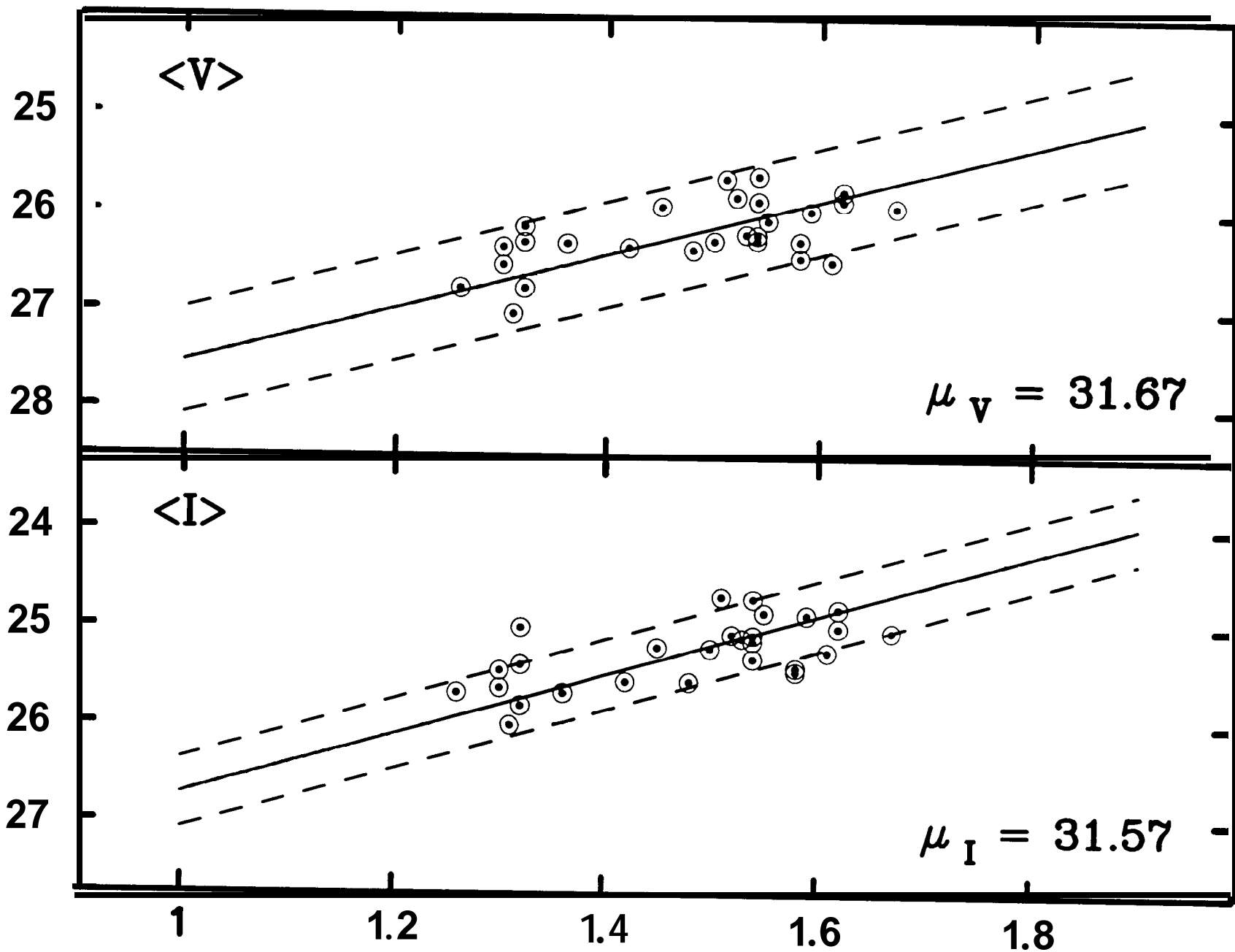
VIRGO



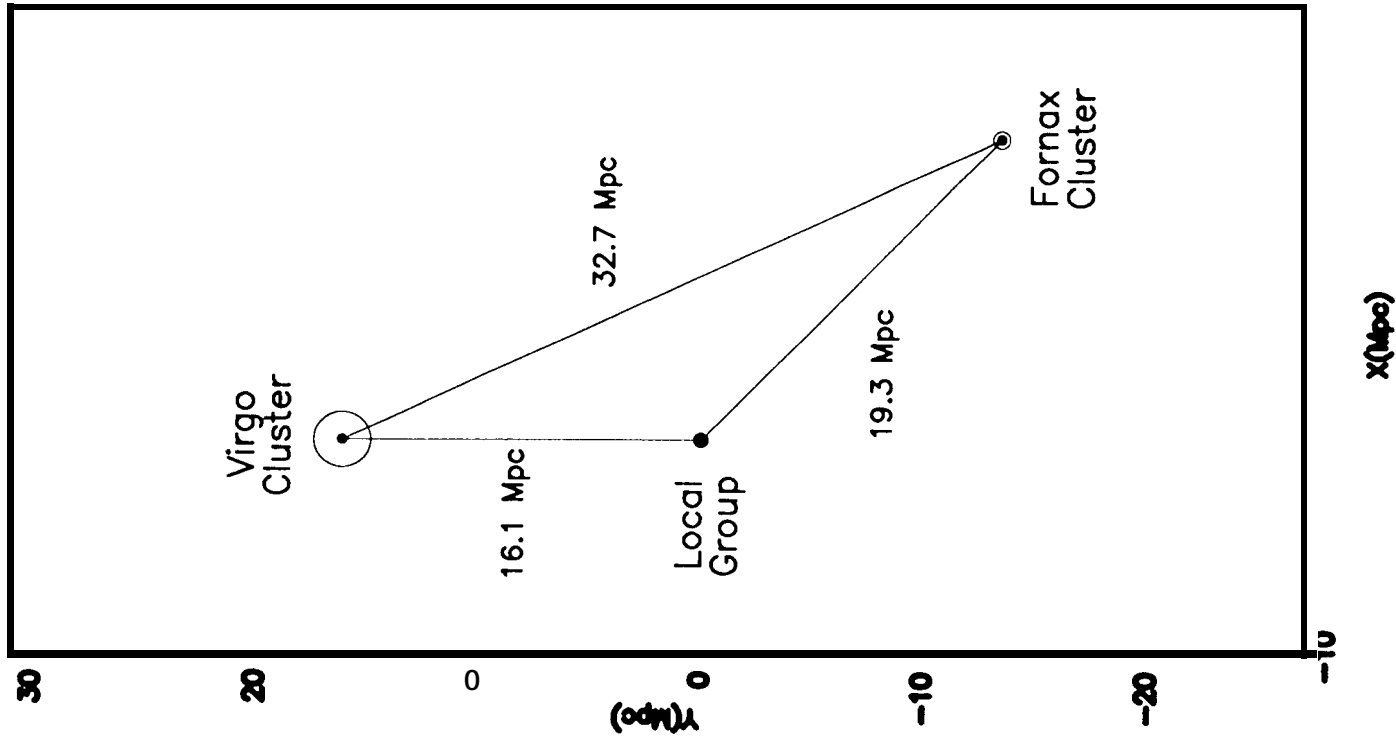




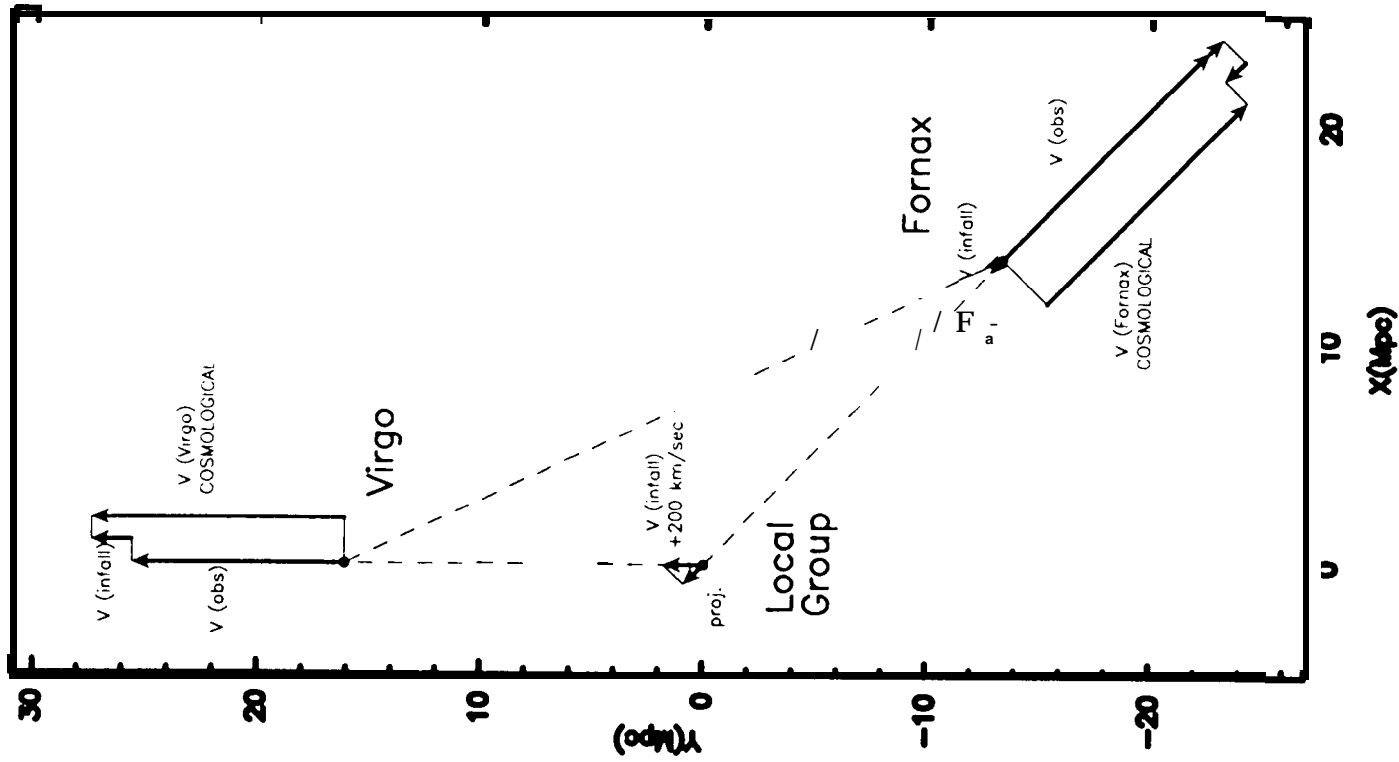
NGC 1365



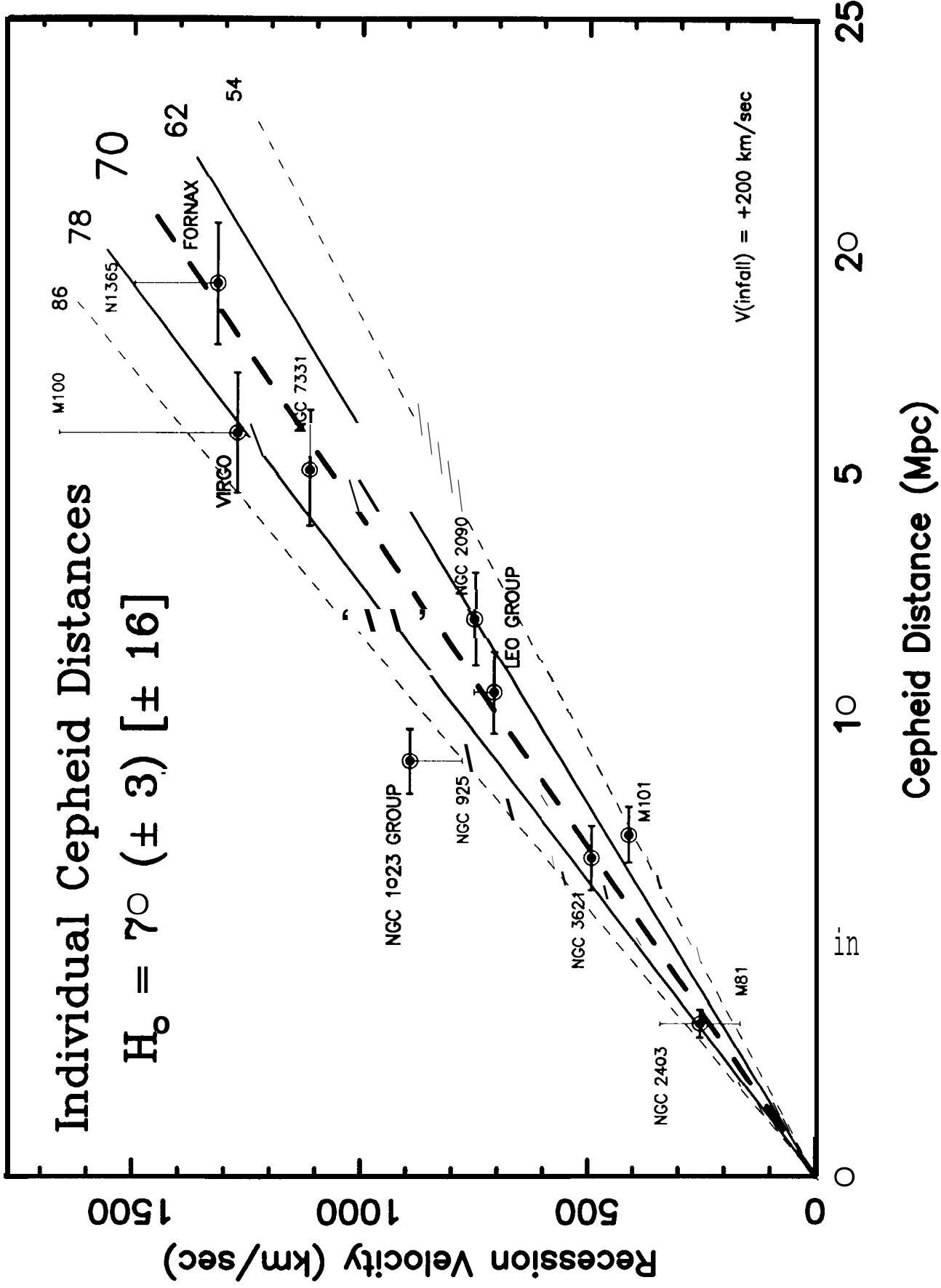
Structure



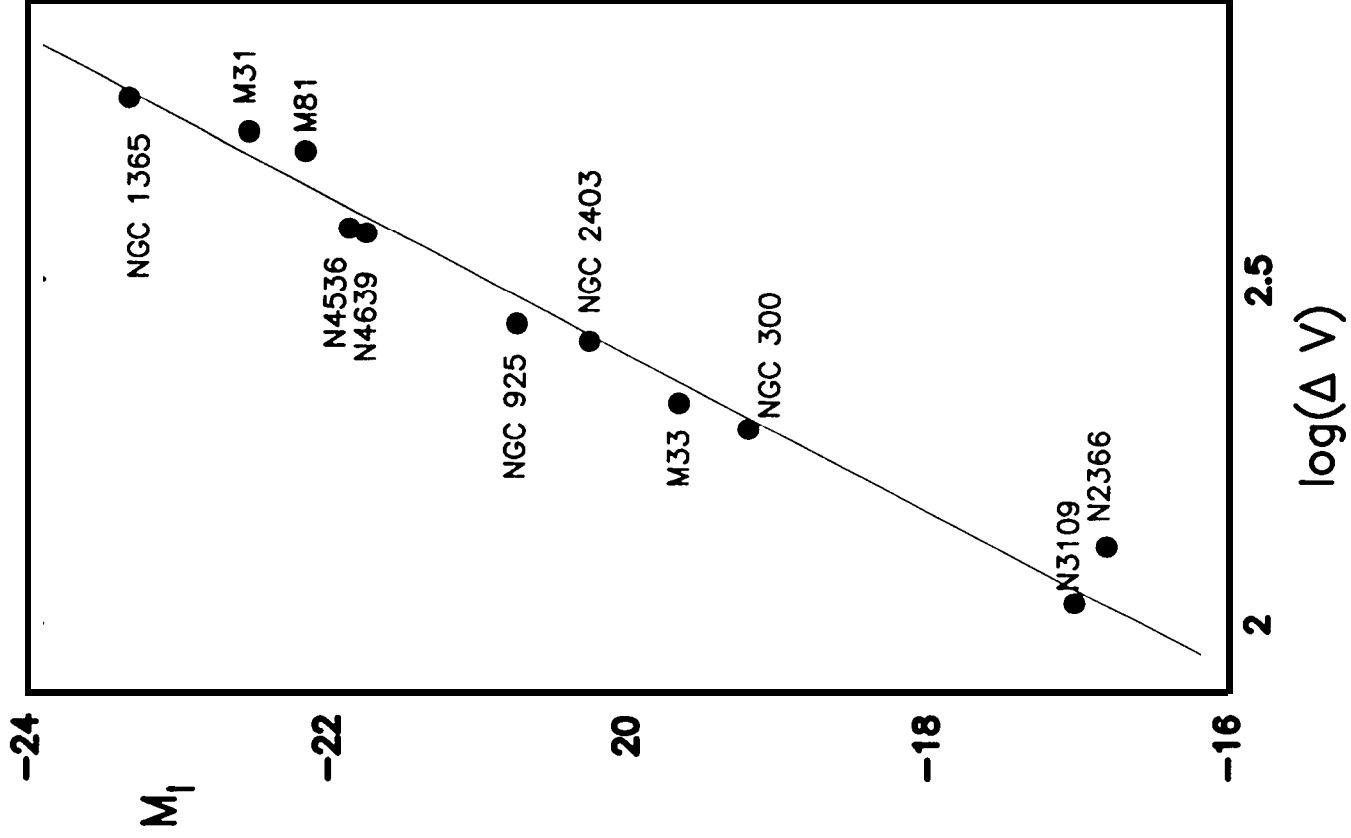
Velocity Field



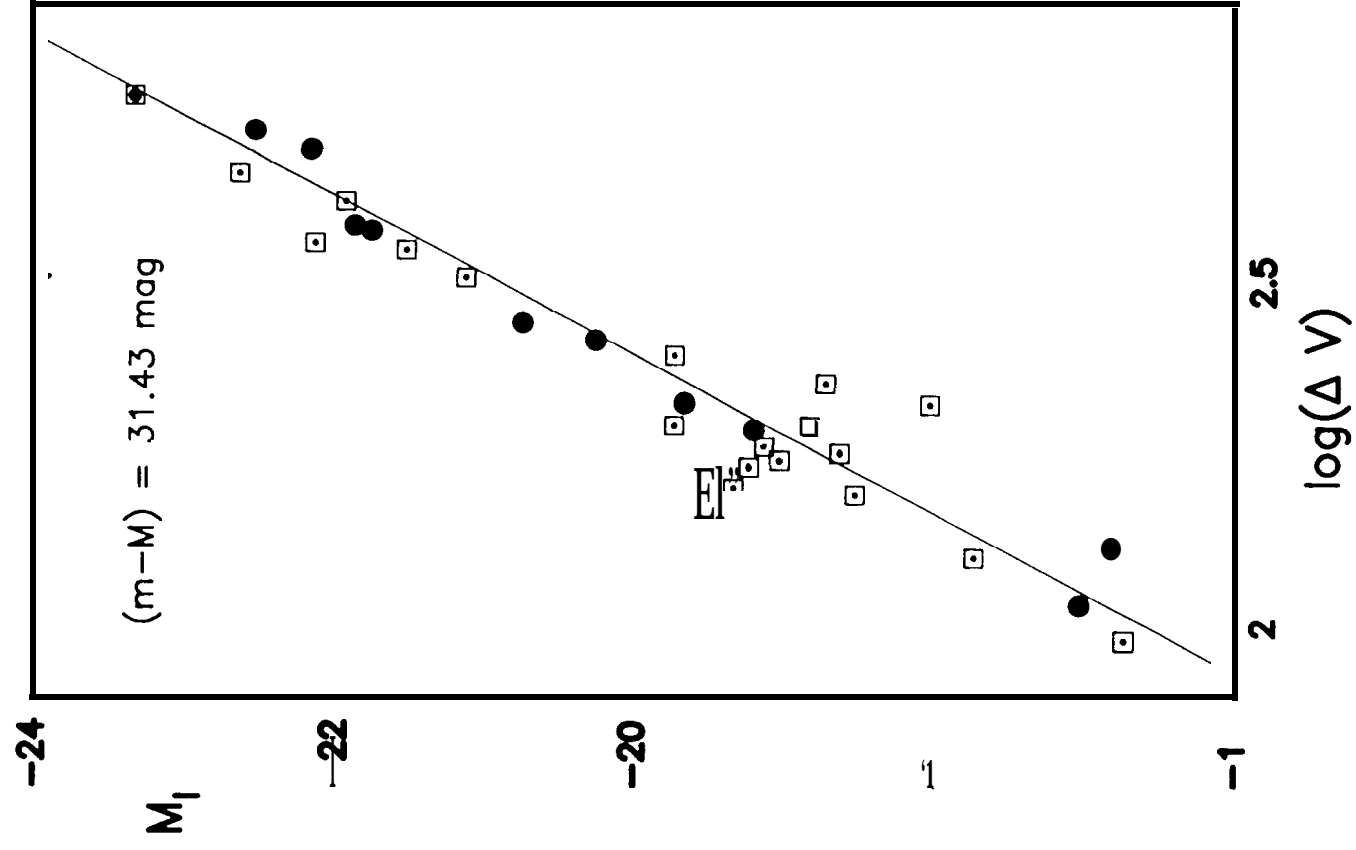
Local Hubble Constant



Cepheid Calibrators



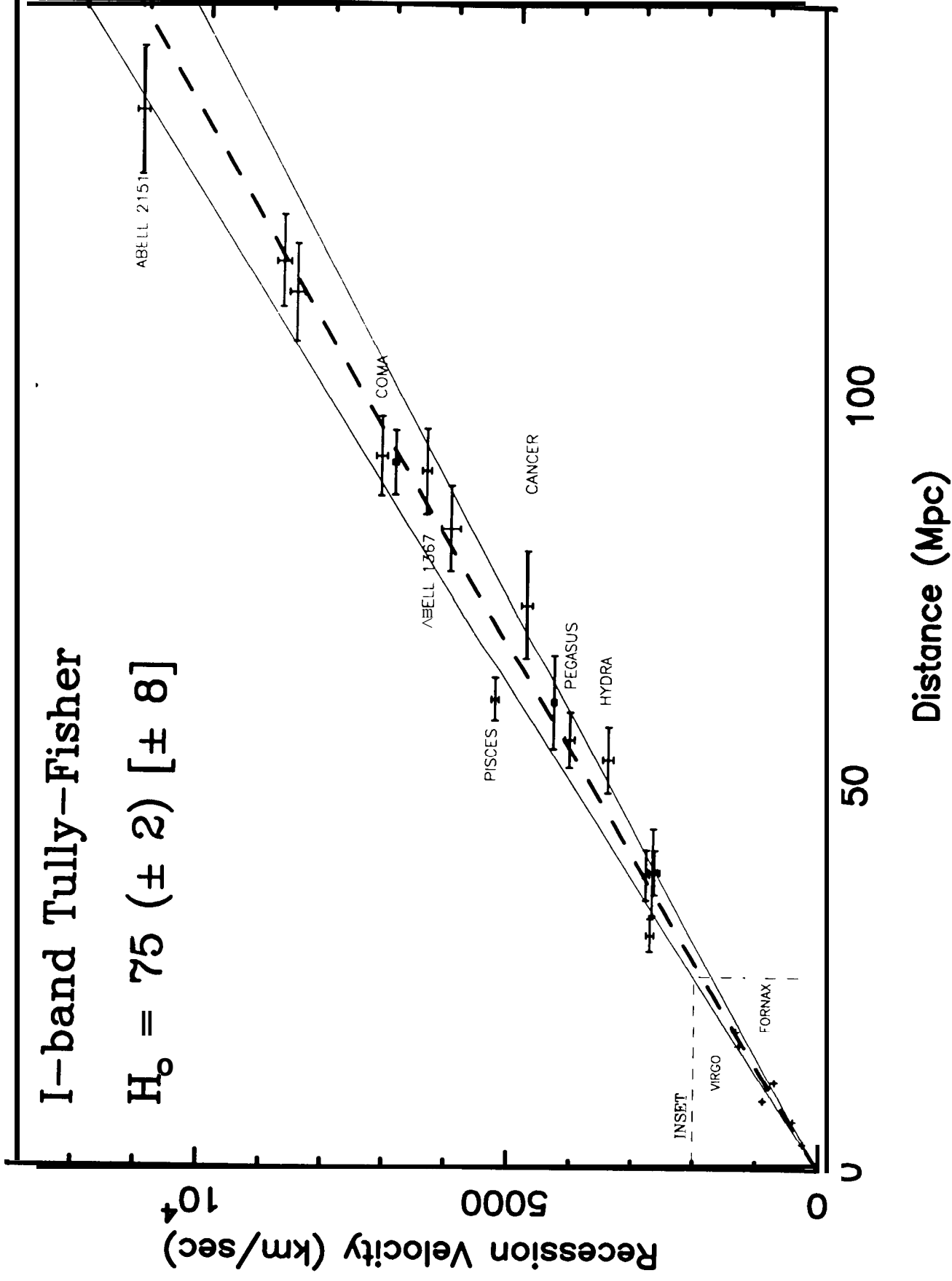
Fornax Galaxies



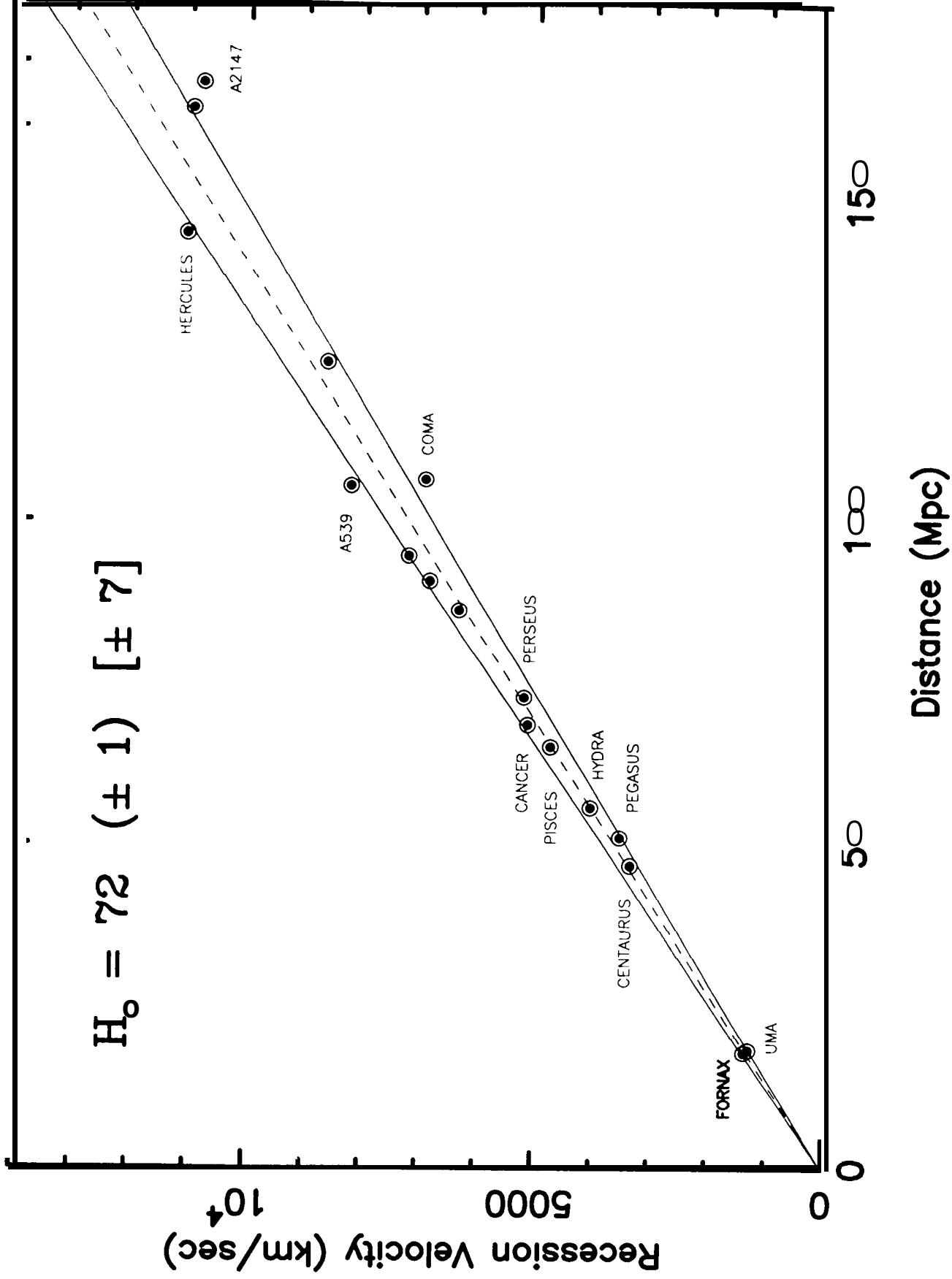
Far-Field Hubble Constant

I-band Tully-Fisher

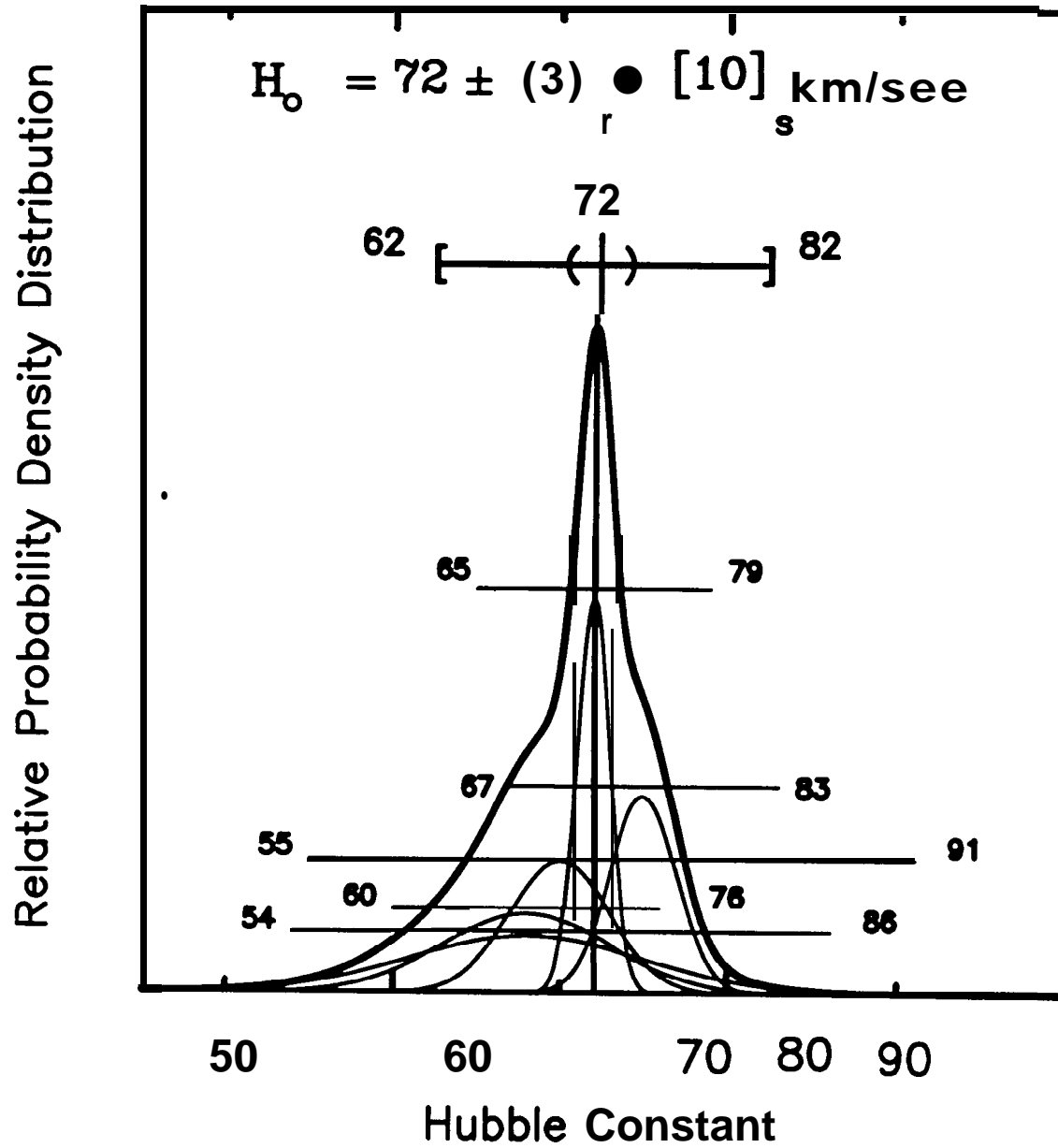
$$H_0 = 75 (\pm 2) [\pm 8]$$



Hybrid Cluster Sample



Hubble Constant Probability Density



Age Constraints

